Effect of Particle Functionalization on Structural and Dielectric Properties of Flexible TPU/BaTiO3/MWCNTs Composite Films

WILEY-VCH

Effect of Particle Functionalization on Structural and Dielectric Properties of Flexible TPU/$BaTiO_3$/MWCNTs Composite Films

E. Stojchevska, R. Popeski-Dimovski, Ž. Kokolanski, C. Gualandi, A.Bužarovska**

E. Stojchevska, A.Bužarovska
Ss Cyril and Methodius University, Faculty of Technology and Metallurgy, Rudjer Boskovic 16, 1000 Skopje, N. Macedonia
E-mail: abuzar@tmf.ukim.edu.mk

R. Popeski-Dimovski
Ss Cyril and Methodius University, Faculty for Natural sciences and Mathematics, Institute of Physics, Arhimedova 3, 1000 Skopje, N. Macedonia

Ž. Kokolanski
Ss Cyril and Methodius University, Faculty of Electrical Engineering and information technologies, Rudjer Boskovic 16, 1000 Skopje, N. Macedonia

C. Gualandi
Department of Chemistry "Giacomo Ciamician" and INSTM UdR of Bologna, University of Bologna, Via Selmi, 2, 40126 Bologna, Italy
E-mail: c.gualandi@unibo.it

Keywords: thermoplastic polyurethane, barium titanate, MWCNTs, surface functionalization, dielectric materials

Abstract

Flexible, low-cost thermoplastic polyurethane (TPU) composite films with functionalized $BaTiO_3$ (BT) and multiwall carbon nanotubes (MWCNTs) are prepared by solution casting method and tested as dielectric materials. Different volume content loadings of BT filler (between 10 and 80 vol%) and 0.12 vol% of MWCNTs are applied. The effects of particle functionalization and BT content on the structural, mechanical and energy storage properties are studied by Fourier infrared spectroscopy (FTIR), differential scanning calorimetry (DSC), as well as puncture and dielectric measurements. It is found that the particle functionalization

and BT content significantly affect the hydrogen bonding within the polymer matrix, and have a huge impact on the mechanical and dielectric properties. The optimal concentration (30 vol% functionalized BT and 0.12 vol% of functionalized MWCNTs) giving the highest dielectric constant of 30.28 and dielectric breakdown strength of 42 kV/mm is determined.

1. Introduction

The rapid development of various technologies for the production of electricity from renewable energy sources has imposed the need for new energy storage devices. Dielectrics, able to store electrical energy as a consequence of polarization under an external electric field, are the core materials of some kinds of energy storage devices, such as capacitors. To achieve high energy storage density, several key parameters, such as high dielectric constants, high breakdown strength, and low dielectric losses, are needed. Following the constant demand, current scientific research is devoted to developing cheap, easily processable and high dielectric constant materials.

In this context, ferroelectric ceramics have already been proven as excellent dielectric materials due to their high dielectric constants and capability of storing a large amount of electricity. However, a wider use of ceramic materials is limited due to their brittleness, relatively low breakdown strength and high dielectric losses. On the other hand, polymers as easy processable materials are characterized by low dielectric losses, high breakdown strength and flexibility, but they possess very low dielectric constants. Consequently, the introduction of ceramic particles into a polymer matrix is a good strategy to integrate the advantages of both materials in order to develop highly flexible composites with desired dielectric properties.[1] Numerous composites based on various polymer ferroelectric matrices, such as poly(vinylidene fluoride) (PVDF), its copolymers and ceramic fillers with high dielectric constants, have been already developed and published.[2-4] In spite of the relatively good characteristics of the ferroelectric polymers, their poor temperature stability and high price were the main reasons to develop composite materials based on non-ferroelectric polymer matrices and high dielectric constant ceramics in high loadings. In this context, various elastic electrically inactive matrices such as poly(dimethylsiloxane), thermoplastic poly(urethanes), etc. have already been employed.[5,6]

Thermoplastic poly(urethanes) (TPUs) are unique, linear block copolymers with high flexibility and excellent mechanical properties such as tensile strength, toughness and elongation at break.[7] The different behaviour in TPUs arises from their dual-phase microstructure based on alternating hard and soft segments, depending on the type of

polyisocyanates, chain extenders and polyols or long polyesters. Therefore, the properties of TPU can be controlled by adjusting the chemical structure and morphology of the segments. This class of material is extensively used to prepare components for flexible devices and has promising dielectric properties according to previous results[8] and density functional theory.[9] Barium titanate ($BaTiO_3$, BT) is a widely used ceramic filler in different composites owing to its high dielectric permittivity and high density. In comparison to all other ceramic fillers based on lead, $BaTiO_3$ is an environmentally friendlier material. The dielectric properties of $BaTiO_3$ were found to be highly affected by its particle size. Huan et al. have revealed that $BaTiO_3$ with an average grain size of around 1μm has increased dielectric constant, piezoelectric coefficient and planar electromechanical coupling factor up to 6079, 519 pC/N and 39.5%, respectively.[10] Opposite to this, a lot of research papers have confirmed increased dielectric properties with decreasing grain size.[3] Besides the particle size, the loading content is an additional important parameter when evaluating the dielectric properties. Dielectric permittivity usually increases with $BaTiO_3$ loadings in corresponding composites, but at the same time, the flexibility and breakdown strength of the polymer matrix significantly decrease. Additionally, the weak interaction between the ceramic filler and the polymer matrix might hamper the proper particle distribution within the polymer matrix and, consequently, the improvement of the dielectric properties of the composite. Thus, numerous efforts have been made to improve the interface between the ceramic filler and the polymer matrix. The introduction of hydroxyl groups on the surface of $BaTiO_3$ particles with proper functionalization treatment promoted the formation of chemical interactions with PVDF matrix, leading to improved dielectric properties of the PVDF/$BaTiO_3$ composites.[11]

The dielectric properties can be further improved by incorporating electrically conductive nanofillers, such as carbon nanotubes (CNTs), graphene and different metal nanoparticles.[12] The main advantage of using conductive CNTs is that a conductive network for charge transfer can be obtained by using a small amount of nanofiller, due to the large surface area and aspect ratio.[13] On the other hand, bare CNTs are easily disposed to aggregation, forming bundles and making them difficult to use. To overcome this problem, proper functionalization of CNTs with different acids introducing surface COOH groups was reported.[14]

The aim of this research was to produce flexible, low-cost, thermoplastic polyurethane/$BaTiO_3$/MWCNTs composite films with improved dielectric properties. The $BaTiO_3$ ceramic filler and multiwall carbon nanotubes (MWCNTs) were properly functionalized in order to promote better dispersion within the TPU polymer matrix and

investigate the possible formation of polymer-particles "network" and its influence on morphological, structural, mechanical and dielectric properties of the final composites.

2. Results and Discussion

2.1. Surface functionalization of $BaTiO_3$ and MWCNTs

The surface functionalization of $BaTiO_3$ and MWCNTs was performed in order to create a network of hydrogen bonds between -OH groups in BT, -COOH groups in MWCNT and urethane groups in TPU, to stabilize the regions at the interface between the different phases, improve the dispersibility of the fillers and enhance the dielectric properties of TPU composite films.

The proper functionalization of MWCNTs was investigated with UV/Vis spectroscopy. **Figure 1**a reports the UV/Vis spectra of MWCNTs before and after nitric acid treatment. The strong absorption peak that appeared at 255 nm was characteristic of MWCNTs chemically modified with HNO_3,[15] thus confirming the presence of attached -COOH groups. The FTIR spectra of unmodified and functionalized $BaTiO_3$ particles are presented in Figure 1b. Two new bands in the spectrum of functionalized $BaTiO_3$ were detected, positioned at 3220 cm^{-1} and 1625 cm^{-1} corresponding to the OH stretching and OH bending vibrations, thus confirming a successful attachment of -OH groups onto the surface of $BaTiO_3$ particles.

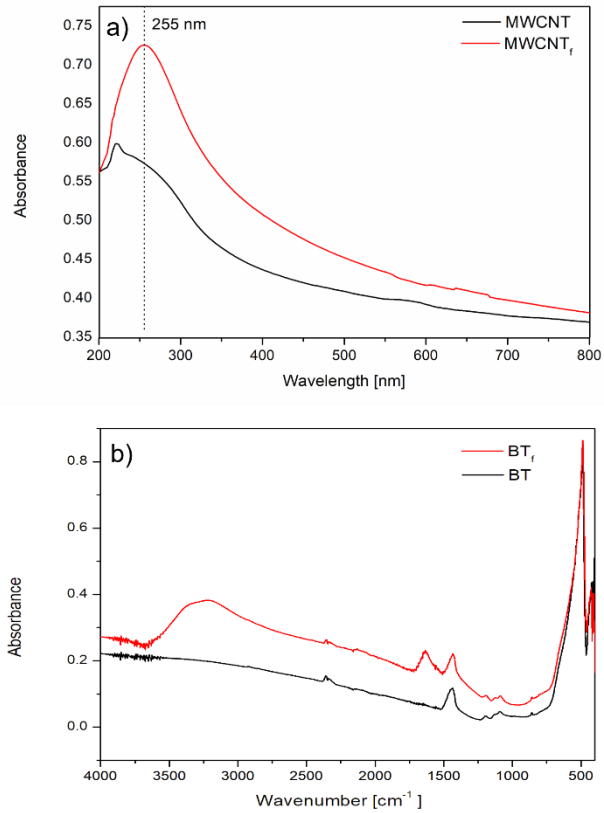

Figure 1. (a) UV/Vis spectra of functionalized MWCNTs and (b) FTIR spectra of functionalized $BaTiO_3$ particles.

2.2. Characterization of composite films

Composite samples with different content of fillers were prepared by solvent casting technique. Two series of composites were prepared: TPU/$BaTiO_3$, and TPU filled with functionalized $BaTiO_3$ and MWCNTs particles (**Table 1**).

Table 1. Samples abbreviation and composition of TPU and its composite films.

Sample code	$BaTiO_3$ [vol%]	MWCNTs [vol%]
TPU	/	/
TPU/BT10	10	/
TPU/BT20	20	/
TPU/BT30	30	/
TPU/BT80	80	/
TPU/BT_f10/$MWCNT_f$	10	0.12
TPU/BT_f20/$MWCNT_f$	20	0.12
TPU/BT_f30/$MWCNT_f$	30	0.12
TPU/BT_f80/$MWCNT_f$	80	0.12

SEM analysis of film cross-sections was carried out to assess the distribution and morphology of the fillers in the polymer matrix. **Figure 2** reports representative sem images of TPU and TPU/BT series (two different magnifications) and of TPU/BT_f/$MWCNT_f$ series (a single high magnification). BT particles can be clearly distinguished from the TPU matrix and their concentration increases according to the feed formulations. BT appear homogeneously distributed across the section as single particles, with diameters in the range 300-500 nm, although few agglomerates with diameters up to 1 µm are present, especially in the composites containing the highest BT amount, in line with the nominal BT dimension provided by the supplier. No remarkable differences can be found between the morphology and the distribution of functionalized and unfunctionalized BT particles, whereas the MWCNTs detection was difficult due to their low concentration.

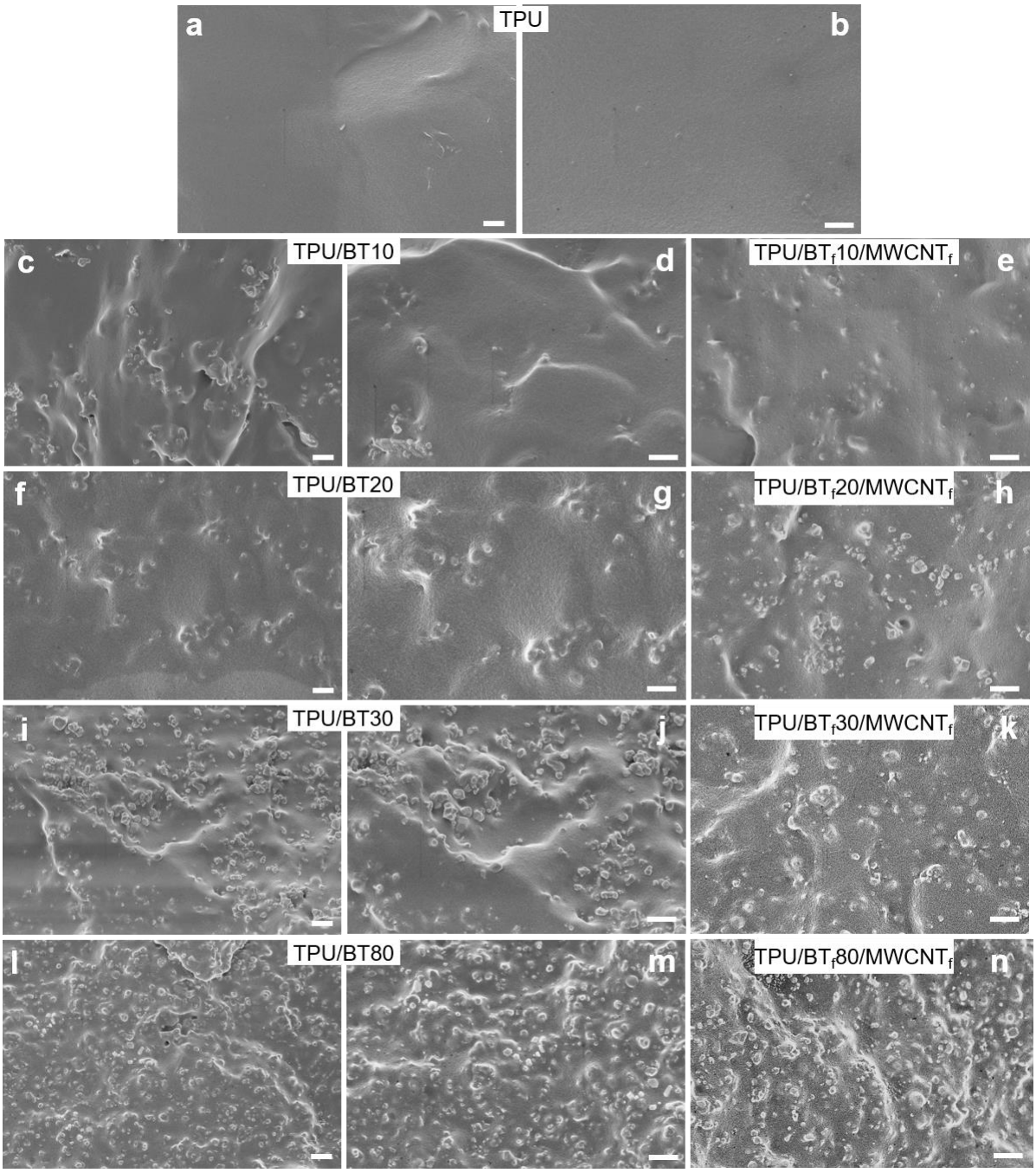

Figure 2. Representative SEM images of sample sections: (a-b) TPU; (c-d) TPU/BT10; (e) TPU/BT$_f$10/MWCNT$_f$; (f-g) TPU/BT20; (h) TPU/BT$_f$20/MWCNT$_f$; (i-j) TPU/BT30; (k) TPU/BTf30/MWCNT$_f$; (l-m) TPU/BT80; (e) TPU/BT$_f$80/MWCNT$_f$. Scale bar = 2 µm.

FTIR analysis of TPU composite films was conducted, aiming to settle possible interactions between the polymer matrix and the functionalized fillers through the evaluation of the hydrogen bonding index (HBI). It is well known that hydrogen bonding in polyurethanes is mainly attributed to the interactions of NH with the carbonyl groups in urethane groups of the hard segments (HS) or interactions with ether groups characteristic of the soft segments (SS).

[16] The recorded spectra of pure TPU and the corresponding composites are shown in **Figure 3**. The spectrum of pure TPU showed an absorption band at 3325 cm^{-1} that was attributed to the hydrogen-bonded N-H stretching vibration in the urethane group.[16] The strong absorption peaks positioned at 2916 cm^{-1} and 2846 cm^{-1} were correlated to the asymmetrical and symmetrical vibrational modes in CH_2 groups, respectively. The absorption band at 1696 cm^{-1} was associated with the hydrogen-bonded carbonyl group, while the peak at 1727 cm^{-1} was related to the free urethane carbonyl (C=O) groups. It could be noted that the incorporation of non-functionalized BT and functionalized BT_f/$MWCNT_f$ particles in the TPU matrix had no pronounced influence on its absorption bands shifting. Nevertheless, the addition of non-functionalized filler and fillers with proper functional groups might alter the hydrogen bonding within the macromolecular chains affecting the final properties. The hydrogen bonding index (HBI) was calculated using Equation 1:[17]

$$\mathrm{HBI} = \frac{A_{\text{bonded C=O}}}{A_{\text{free C=O}}} \qquad [1]$$

where $A_{\text{bonded C=O}}$ and $A_{\text{free C=O}}$ are the integrated areas of absorption peaks located at 1697 cm^{-1} and 1727 cm^{-1}, respectively.[17] As these two peaks were not well separated, curve fitting with Gaussian function was performed using Origin 8.1 software (Inset in Figure 3a). Greater values of HBI indicate increased participation of the carbonyl group to the hydrogen bonding. The calculated HBI indices for pure TPU and its composites are collected in **Table 2**. It is evident that the estimated HBI indices for both series of composite films were higher than the HBI index of TPU and increased with increasing the amount of the fillers. This result suggests that the presence of fillers promotes the formation of hydrogen bonding, no matter whether they are functionalized or not. It is worth noting that in the TPU/BT_f/$MWCNT_f$ composite films (Figure 3b) the HBI indices were generally lower when compared to those of TPU/BT system at the same $BaTiO_3$ concentration. A trivial explanation of this result cannot be found, given that the presence of $MWCNT_f$ may affect also the HBI indices. In the case of TPU with unfunctionalized BT, it can be assumed that hydrogen bondings concentrate only on the polymer matrix and that an increasing amount of BT may induce densification of polymer chains to better promote polymer-polymer interaction and free-volume decrease, thus resulting in an HBI increase. Differently, by using functionalized fillers, hydrogen bonds can be established at the polymer-particle interface, thus reducing the tendency of the chain to segregate from the particles.[18]

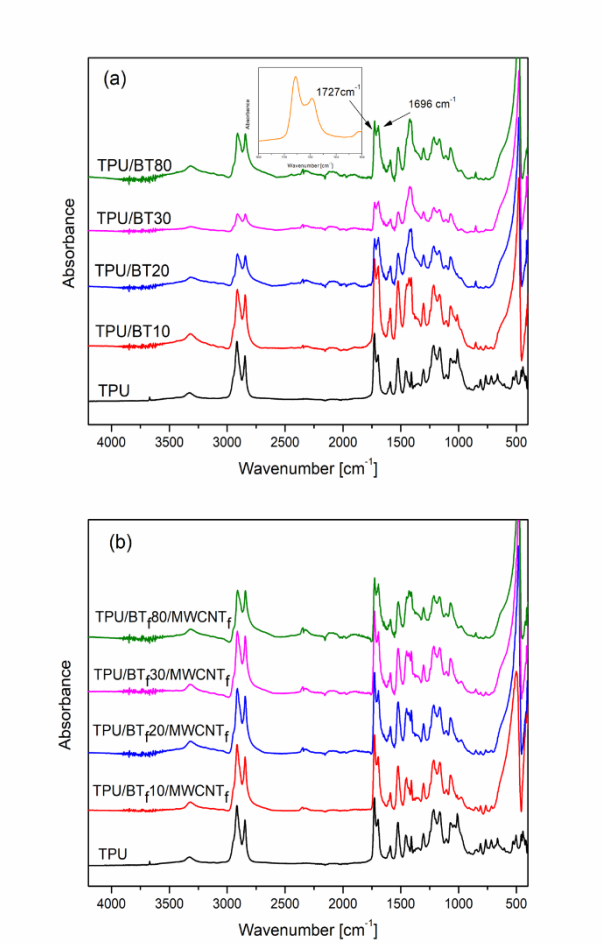

Figure 3. FTIR spectra of (a) TPU/BT and (b) TPU/BT_f/$MWCNT_f$ composite films. Inset in (a) curve-fitted peaks located at 1727 cm^{-1} and 1696 cm^{-1}.

Table 2. Integrated areas of curve fitted peaks at 1696 cm^{-1} and 1727 cm^{-1} and hydrogen bonding indices (HBI) for TPU, TPU/BT and TPU/BT_f/$MWCNT_f$ composite films.

Sample	Peak 1696 cm^{-1}	Peak 1727 cm^{-1}	HBI[a)]
TPU	3.49	4.31	0.81
TPU/BT10	5.77	7.0	0.82
TPU/BT20	4.95	3.17	1.56
TPU/BT30	3.40	1.99	1.70
TPU/BT80	7.63	3.66	2.08
TPU/BT_f10/$MWCNT_f$	5.63	5.92	0.95
TPU/BT_f20/$MWCNT_f$	7.08	5.93	1.19
TPU/BT_f30/$MWCNT_f$	7.20	5.91	1.21
TPU/BT_f80/$MWCNT_f$	7.17	4.09	1.75

[a)] calculated by applying Equation 1.

DSC heating curves recorded for the pure TPU and its composite films are shown in **Figure 4**. The existence of two glass transition temperatures can be observed: the lower glass transition T_{g1} is related to the SS, and the higher glass transition T_{g2} is ascribable to the HS of TPU.[19] Since TPU is a completely amorphous polymer, no visible melting endotherms were detected. The summarized DSC data of the performed measurements are listed in **Table 3**. In TPU/BT films the T_{g1} increased with the increased content of BT, while the T_{g2} values were constant. The increased T_{g1} values indicated a reduction of chain mobility in soft segments. In these composite films, the ceramic filler does not possess any functional groups and therefore the restricted chain mobility in SS cannot be ascribed to polymer-particle interactions. A possible explanation is that the addition of unfunctionalized BT promotes polymer-polymer interaction and free volume reduction, thus initiating more intimate contact between the TPU macromolecules and resulting in restricted chain mobility.[16] In TPU/BT_f/$MWCNT_f$ composite films, the T_{g1} values were almost constant with the increased content of functionalized BT, but significantly lower when compared to the T_{g1} values relevant for TPU/BT systems. Additionally, a slight decrease in the second T_{g2} values could be noted with the increase in BT loadings. The reason for such a behaviour might be due to the participation of both fillers in the formation of hydrogen bonding, causing possible perturbing the strong interactions in urethane groups.[17] These results perfectly corroborate with those obtained from the FTIR analysis.

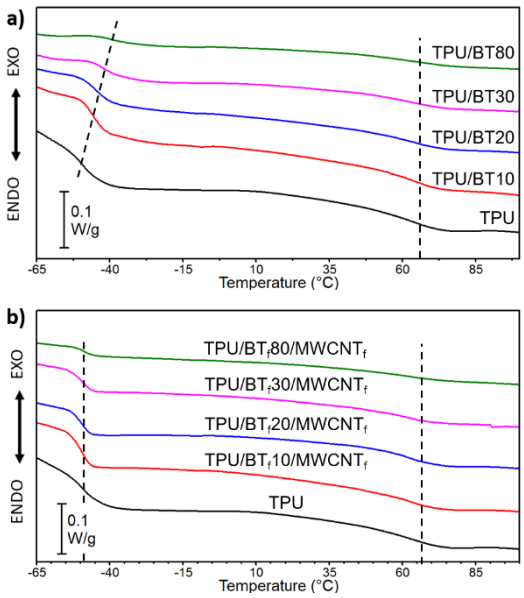

Figure 4. DSC thermograms of (a) TPU/BT and (b) TPU/BT_f/$MWCNT_f$ composite films.

Table 3. Calorimetric data and results of puncture test of TPU, TPU/BT and TPU/BT$_f$/MWCNT$_f$ composite films.

Sample	T_{g1} [ºC]	ΔC_{p1} [$Jg^{-1}C^{-1}$]	T_{g2} [ºC]	ΔC_{p2} [$Jg^{-1}C^{-1}$]	ε [%]	σ [kPa]
TPU	-49	0.21	63	0.114	29.90 ± 0.03	361.6 ± 40.3
TPU/BT10	-46	0.19	64	0.108	36.100 ± 0.004	675.7 ± 11.1
TPU/BT20	-45	0.15	64	0.077	27.200 ± 0.003	783.9 ± 15.1
TPU/BT30	-40	0.11	64	0.067	15.60 ± 0.04	970.3 ± 13.7
TPU/BT80	-38	0.048	64	0.040	1.400 ± 0.003	1381.2 ± 47.0
TPU/BT$_f$10/MWCNT$_f$	-50	0.19	65	0.103	15.90 ± 0.03	486.0 ± 23.0
TPU/BT$_f$20/MWCNT$_f$	-50	0.14	63	0.092	11.500 ± 0.007	651.5 ± 21.1
TPU/BT$_f$30/MWCNT$_f$	-50	0.13	60	0.077	8.300 ± 0.002	736.9 ± 41.3
TPU/BT$_f$80/MWCNT$_f$	-50	0.05	61	0.065	1.400 ± 0.005	990.8 ± 32.2

The results obtained from the puncture measurements of the polymer composite films are summarized in Table 3. It is evident that the puncture elongation decreased with the increased content of the fillers. This was not surprising, taking into account the high volume content of inorganic phase, contributing to increased brittleness of the polymer films.[20] It is interesting to note that lower elongation values were determined for TPU/BT$_f$/MWCNT$_f$ composite films when compared to TPU/BT composites, probably because of the formed "network" between the polymer matrix and the fillers, reducing the elasticity of the systems. In both series of TPU composite films, the puncture strength increased with the increase of BT content. However, the puncture strength values for TPU/BT$_f$/MWCNT$_f$ composites are lower compared to those of TPU/BT composite films at the same BT concentration. Such a behaviour nicely corroborates with the higher HBI indices in TPU/BT systems determined by FTIR spectroscopy.

2.2. Dielectric measurements

Figure 5 and 6 show the frequency dependence of the dielectric constant (ε_r) and dielectric loss (tan δ) of the neat TPU and its composite films. It can be seen that the ε_r of both series of composites displayed almost no correlation to frequency. The recorded dielectric constants of all investigated samples at 1 MHz are summarized in **Table 4**. The dielectric constant for the neat TPU was 7.26 which was approximate to the reference literature values.[21] Furthermore,

ε_r of TPU/BT composite films increased with the addition of BT, but these obtained results were lower than expected, taking into account the high volume of ceramic loadings. These observed results could be due to the grain size of BT particles, which directly affects the dielectric properties of the composite.[5,22] On the other hand, the composite films with modified fillers showed an increasing trend of ε_r, as soon as the BT_f content was within 30 vol%, thus confirming the indications that the dielectric properties are largely dependent on the polymer matrix/filler interactions.[23] Surprisingly, the ε_r of the composite film filled with 80 vol% BT_f (TPU/BT_f80/$MWCNT_f$) was comparable to that of pure TPU. To confirm if there is a decreasing trend of ε_r for filler loadings higher than 30 vol%, two TPU films with 40 and 60 vol % of functionalized BT_f and 0.12 vol% of $MWCNT_f$ as fillers were additionally produced. The dielectric constant of TPU/BT_f30/$MWCNT_f$ was equal to 30.28 at 1 MHz, but as can be seen in Figure 5b, for TPU/BT_f40/$MWCNT_f$ and TPU/BT_f60/$MWCNT_f$ the dielectric permittivity drops to 19.68 and 12.08, respectively. Consequently, it can be concluded that the optimal concentration of fillers for this type of composite film is 30 vol% of BT_f and 0.12 vol% of $MWCNT_f$. It is obvious that the dielectric response increased in TPU/BTf/MWCNTs composite films, but not as expected. Although MWCNTs exhibit high value of the dielectric constant and increased electrical conductivity, their functionalization and interactions with functionalized BT particles and TPU urethane groups diminish these effect.

The dissipation factor is an important property for materials intended for capacitors, and ideally, materials for this type of application require the lowest possible dielectric losses.

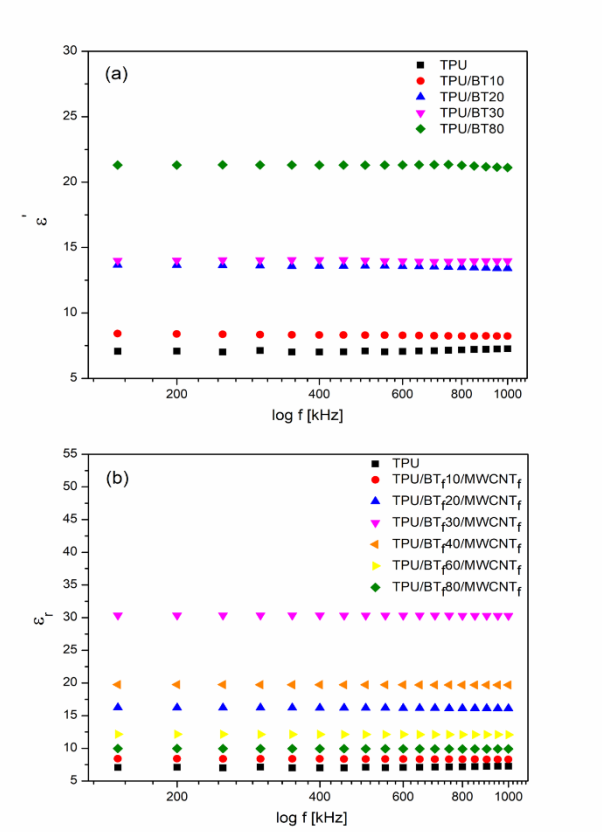

Figure 5. Frequency dependence of the dielectric constant ε_r in (a) TPU/BT and (b) TPU/BT_f/$MWCNT_f$ composite films.

Table 4. Dielectric constant (ε_r), dielectric loss (tan δ), average breakdown voltage (U_b), average thickness (d) and dielectric breakdown strength (E_b) of TPU, TPU/BT and TPU/BT_f/$MWCNT_f$ composite films.

Sample	ε_r	tan δ	U_b [kV]	d [mm]	E_b [kV/mm]
TPU	7.26	0.325	5.43 ± 0.6	0.097	56.0 ± 6.2
TPU/BT10	8.22	0.223	6.75 ± 0.3	0.099	68.18 ± 3.5
TPU/BT20	13.41	0.198	7.00± 0.1	0.101	70.29 ± 1.4
TPU/BT30	13.97	0.174	6.80 ± 0.2	0.096	70.83 ± 2.8
TPU/BT80	21.11	0.082	5.30 ± 0.1	0.188	28.19 ± 2.3
TPU/BT_f10/$MWCNT_f$	8.29	0.038	3.73 ± 0.1	0.093	40.14 ± 1.2
TPU/BT_f20/$MWCNT_f$	16.10	0.033	3.78 ± 0.1	0.097	39.0 ± 1.0
TPU/BT_f30/$MWCNT_f$	30.28	0.031	4.12 ± 0.3	0.098	42.09±3.9
TPU/BT_f80/$MWCNT_f$	9.89	0.018	5.10 ± 0.4	0.152	33.55 ± 3

In contrast to the dielectric constant, the dielectric loss of all TPU films showed frequency dependence, especially for TPU/BT films, as shown in **Figure 6**.[21] As it can be seen from Table 4, both series of TPU films exhibited reduced dielectric losses with the addition of BT, however, lower values were found for TPU films with modified fillers, which indicated that the incorporation of a specific quantity of $MWCNT_f$ can increase the dielectric constant and decrease the loss tangent.[5,24]

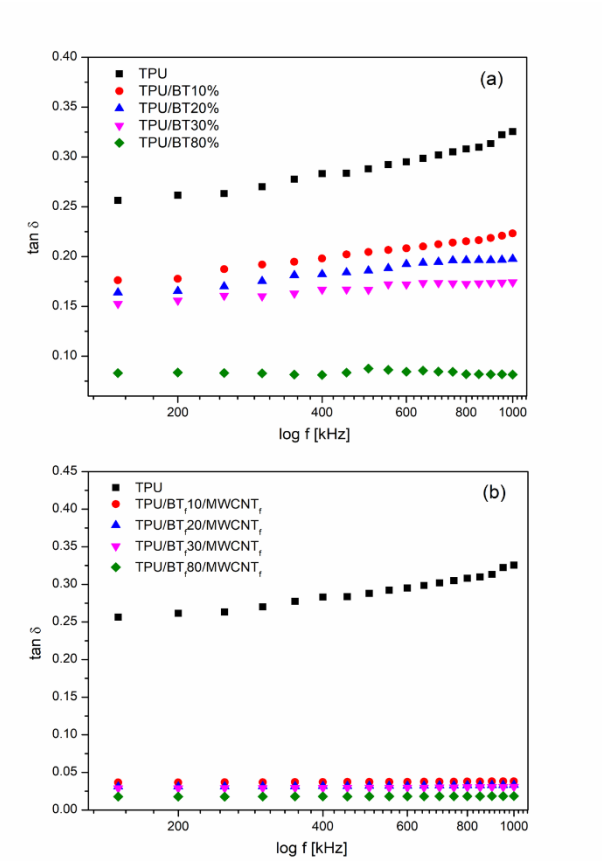

Figure 6. Frequency dependence of the dielectric losses (tan δ) on (a) TPU/BT and (b) $TPU/BT_f/MWCNT_f$ composite films.

One of the basic requirements for the application of dielectric materials in capacitors is to possess resistivity to higher electric fields. To examine this behavior, the dielectric breakdown strength (E_b) of the TPU composite films was analyzed by measuring the breakdown voltage. The obtained results for dielectric breakdown strength, summarized in Table 4, showed relatively high values.[25,26] The variations of E_b with the $BaTiO_3$ content, for both types of composites, are shown in **Figure 7**. It could be seen that the breakdown strength of the TPU/BT composite films (Figure 7a) showed an expected increasing trend with the addition of $BaTiO_3$ filler, while a sharp drop in its value was determined for TPU/BT80 composite. This drastic reduction of E_b at a high volume fraction of $BaTiO_3$ might be due to the fact that

high ceramic filler loadings lead to more defects and voids, increasing the risk of failure.[27,28] However, the E_b values of the composite films filled with modified fillers exhibited an irregular and decreasing trend (Figure 7b), mainly as a result of the addition of MWCNTs, making the polymer matrix conductive.[29] Nevertheless, the obtained dielectric breakdown strength values remained relatively high, since the functionalized $BaTiO_3$ particles retained the insulating properties of the composite films.

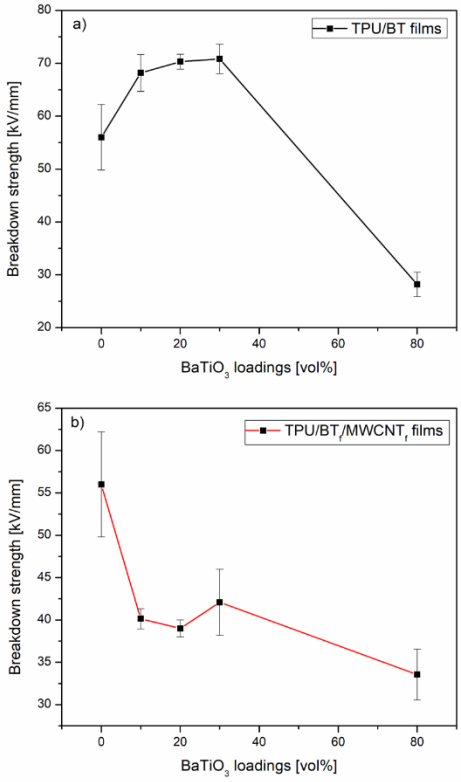

Figure 7. Breakdown strength of (a) TPU/BT and (b) TPU/BT_f/$MWCNT_f$ composite films as a function of $BaTiO_3$ concentration.

3. Conclusion

Thermoplastic polyurethane composite films with functionalized $BaTiO_3$ and MWCNTs fillers were prepared by solution casting method and characterized for potential energy storage applications. Functionalization of BT particles with -OH groups and of MWCNTs with -COOH groups was confirmed by FTIR and UV/VIS spectroscopy, respectevely. Albeit the functionalization of BT and MWCNTs did not significantly affect the morphology and the distribution of the particles, it had a high influence on the hydrogen bonding index (HBI) and on composite thermal transitions, in particular on the mobility of the chain soft segments. Significantly increased puncture strengths (up to 990 kPa) and lower elasticity were achieved

with the increase of BT filler content. The highest dielectric permittivity of 30.28 and satisfactory dielectric breakdown strength of 42 kV/mm were achieved in the composite containing 30 vol% of functionalized $BaTiO_3$. The overall results of TPU/BT and TPU/BTf/MWCNTf composite films are promising for designing new energy storage dielectrics with high flexibility.

4. Experimental section

Materials: bio-based thermoplastic polyurethane (M_n = 160 kDa, PDI = 6), synthesized and characterized in a previous work, was used as a polymer matrix.[30] $BaTiO_3$ (BT) powder (purity ≥ 99%), with a nominal particle size in the range of 0.85 - 1 µm, was purchased from Acros Organics. NC7000 MWCNTs (90%) were supplied by NANOCYL S.A. (Belgium), with average length and diameter of 1.5 mm and 9.5 nm, respectively. Chloroform (purity ≥ 99%), used as a solvent, was supplied by Sigma Aldrich. Hydrogen peroxide (30%), nitric acid (%) and ethanol (purity ≥96 %) were products of Alkaloid, Skopje. All chemicals were used as received without previous purification.

Functionalization of $BaTiO_3$ and MWCNTs: a proper amount of BT powder was mixed with hydrogen peroxide solution (30%) and refluxed at 110 °C for 5 h. Subsequently, the sample was rinsed with distilled water, filtered and dried at 80 °C for 24 h. The functionalization of MWCNTs was performed using 3 M nitric acid under reflux, for 24 h at 80 °C, followed by rinsing, centrifugation and drying in oven at 80 °C.

Composite films preparation: for preparing TPU/BT series of composite, TPU was dissolved in chloroform (5 wt%) at room temperature (RT) for 24 h. Then, appropriate amount of BT powder was added to the solution, sonicated with a Bandelin Sonopuls ultrasonic homogenizer and then the prepared solutions were cast onto Petri dishes (d = 5 cm) and dried at RT. For preparing TPU/BT_f/$MWCNT_f$ the functionalized particles at proper contents were mutually ultrasonically treated in ethanol for 30 min and then dried at 60 °C. The obtained mixtures were then ground and dispersed in TPU solutions, as it was described for TPU/BT composites.

Characterization: Infrared spectroscopy was carried out with a Fourier Infrared (FTIR) Shimadzu IRAffinity-1S spectrometer by recording 32 scans in the range of 4000 - 400 cm^{-1}, with a resolution of 4 cm^{-1}. The UV/VIS absorption spectroscopy was carried out with Hewlett Packard 8452A diode Array Spectrometer (USA). Scanning electron microscopy (SEM) was performed on a Zeiss LEO 1530 FE-SEM, operated at 5 kV. Samples were sputter-coated with gold before SEM observations. And observed with an In-lens SE detector.

Differential Scanning Calorimetry (DSC) was carried out using a Q2000 DSC apparatus (TA instruments) equipped with a Refrigerated Cooling System (RCS90). Samples were subjected to a first heating scan in the temperature range -90-110 °C at a rate of 20 °C min^{-1}, followed by a controlled cooling at 20 °C min-1 to -90 °C and a second heating scan at 20 °C min^{-1} to 110 °C. The glass transition temperatures (T_g) were taken at half-height of the glass transition heat capacity steps. Puncture properties were measured using a TA.XT. Plus-Stable Micro System (UK). The analyzed samples with dimensions 15 mm x 15 mm were fixed on a perforated platform with duct tape. A 2 mm diameter probe was used to punch the squared samples in the centre with a speed of 1 mm s^{-1}. The average puncture strength (σ) and elongation (ε) were taken as averaged values of five measurements per sample. The dielectric properties of the samples were measured by Impedance analyzer, Keysight E4990A and Keysight 16451B Dielectric Test Fixture with electrode B (d = 5 mm), in a frequency range of 20 Hz to 20 MHz with basic accuracy of 0.045% (typ.). The 16451B is a Dielectric Test Fixture used with impedance analyzers for accurate measurement of insulating and dielectric materials. The 16451B employed the parallel plate method, which sandwiches the material between two electrodes to form a capacitor. An impedance analyzer is then used to measure the capacitance. The dielectric constant of the samples was calculated as follows:

$$\varepsilon_r = \frac{c_p}{\varepsilon_0}\frac{t_a}{A} \qquad [2]$$

where ε_0 is the permittivity in vacuum (8.85×10^{-12} F m^{-1}), t_a is the average thickness of the test material [m], A is the area of Guarded electrode [m^2] and C_p is the equivalent parallel capacitance [F]. Additionally, the dielectric dissipation factor (tan δ) was measured and the obtained results were the actual values of dielectric loss for TPU composites. Dielectric breakdown strengths were measured using a homemade breakdown voltage generator, operating with a direct electric signal, with a voltage up to 6 kV and a maximum electric current of 10 mA. Test spikes from the instrument were placed on a randomly selected surface on both sides of the test specimens. The measurement of the breakdown voltage of each sample was performed three times, and the declared measured value was calculated as the average value. The measurements were performed at RT and relative humidity of 54%. The measuring instrument allows a continuous increase of the test voltage with a step of approximately 10 V until the breakthrough voltage was reached, when it was automatically switched off and the result was displayed on the indicator. The declared accuracy of the instrument in the measurement area of 6 kV is:

$$\Delta = \pm|1{,}5\ \%\ U_b + 2\mathrm{dig}| \qquad [3]$$

where U_b is the value displayed on the indicator of the instrument, while "dig" represents the resolution of the instrument (which is 10 V). The obtained results for dielectric strength were then calculated by dividing the breakdown voltage by the thickness of the sample. The data is expressed in kV mm^{-1}. The measurements were performed with a variation of the effective voltage value of the electrical distribution network of less than 2%.

Acknowledgements

This work was financially supported by NATO grant - Project number NATO SPS G5772.

Received: ((will be filled in by the editorial staff))

Revised: ((will be filled in by the editorial staff))

Published online: ((will be filled in by the editorial staff))

References

[1] H.Prashanth, P.V. Shanmugasundram, E. Jayamani, K. H. Soon, *Renew. Sustain. Energy. Rev*. **2022**, *157*, 112075.

[2] B. Fan, M. Zhou, C. Zhang, Y. Liu, D. He, J. Bai, *Mater. Res. Express*. **2019,** *6*, 075071.

[3] Y. Niu, K.Yu, Y. Bai, H. Wang, *IEEE Trans. Ultrason. Ferroelectr. Freq. Control*, **2015,** *62*,108.

[4] A. Bužarovska, M. Kubin, P. Makreski, M. Zanoni, L. Gasperini,·G. Selleri, D. Fabiani, C. Gualandi, *J. Polym.Res*. **2022**, *29*, 272.

[5] C. Nawanil, P. Panprom, K.Khaosa-Ard, W.Makcharoen, N.Vittayakorn, *AIP Conf. Proc*. **2018**, *2010*, 020029.

[6] M.Baibarac, A. Nila, I. Smaranda, M.Stroe, L. Stingescu, M. Cristea, R. C. Cercel, A. Lorinczi, P. Ganea, I. Mercioniu, R. Ciobanu, C. Schreiner, R.G. Garcia, C. Bartha, *Materials* **2021**, *14*, 1.

[7] S. Nayak, B. Sahoo, T. Kumar Chaki, D. Khastgir, *RSC Adv*. **2013**, *3*, 2620.

[8] S. Liu, R. Duan, S. He, H. Liu, M. Huang, X. Liu, W. Liu, C. Zhu, *React. Funct. Polym.* **2022**, *181*, 105420.

[9] R. G. Lorenzini, W. M. Kline, C. C. Wang, R. Ramprasad, G. A. Sotzing, *Polymer* **2013**, *54*, 3529.

[10] Y. Huan, X. Wang, J. Fang, L. Li, *J. Eur. Ceram. Soc.* **2014**, *34*, 1445.

[11] T. Zhou, J. W. Zha, R.Y. Cui, B.H. Fan, J.K. Yuan, Z.M. Dang, *ACS Appl. Mater. Interfaces* **2011**, *3*, 2184.

[12] H. Y. Wang, Y. bin You, J. W. Zha, Z. M. Dang, *Compos. Sci. Technol.* **2020**, 200, 108405.

[13] K. Dash, N. K. Hota, B. P. Sahoo, *J. Mater. Sci.* **2020**, *55*, 12568.

[14] L. Shao, G. Tobias, C.G. Salzmann, B. Ballesteros, S.Y. Hong, A. Crossley, B.G. Davis, M.L.H. Green, *Chem. Commun.* **2007**, *1*, 5090.

[15] W. Zhimin, L.Qingchun, Z. Hui, L.Hanfan, C. Yongming, Y. Mingshu, *Carbon* **2007**, *45*, 285.

[16] F. Şen, E. Baştürk, B. Karadoğan, S. Madakbaş, M. V. Kahraman, *Polym. - Plast. Technol. Eng*. **2016**, *55*, 1325.

[17] B. Molki, W. M. Aframehr, R. Bagheri, J. Salimi, *J. Memb. Sci*. **2018**, *549*, 588.

[18] Y. Sun, J. Teng, Y. Kuang, S. Yang, J. Yang, H. Mao, Z. Gu, *Front. Bioeng. Biotechnol.* **2022**, *10*, 1.

[19] C. Bueno-Ferrer,E. Hablot, F. Perrin-Sarazin, M. C. Garrigós, A. Jiménez, L. Averous, *Macromol. Mater. Eng*. **2012**, *297*, 777.

[20] A. Bužarovska, G. Bogoeva-Gaceva, R. Fajgar, *J. Polym. Eng.* **2016**, *36*, 181.

[21] M. N. Khan, N. Jelani, C. Li, J. Khaliq, *Ceram. Int.* **2017**, *43*, 3923.

[22] M. C. Cheung, H. L. W. Chan, C. L. Choy, *J. Mater. Sci*. **2001**, *36*, 381.

[23] M. T. Sebastian, H. Jantunen, *Int. J. Appl. Ceram. Technol*. **2010**, *7*, 415.

[24] A. S. M. Iftekhar Uddin, D. Lee, C. Cho, B. Kim, *Coatings* **2022**, *12*, 77.

[25] Z. Luo, L. Zhang, Y. Liang, S. Wen, L. Liu, *Polym. Test*. **2022**, 111, 107592.

[26] [24] I. Nurul, J. Mariatti, Polym. Eng. Sci. **2018**, *58* E36.

[27] X.He, J. Zhou, L. Jin, X. Long, H. Wu, L. Xu, Y. Gong, W. Zhou, *Materials* **2020**,*13*, 1.

[28] Z. Pan, L. Yao, J. Zhai, B. Shen, H. Wang, *Compos. Sci. Technol*. **2017**, *147*, 30.

[29] R. Han, Y. Liu, J. Shi, G. X. Chen, Q. Li, *E-Polymers* **2021**, *21*, 272.

[30] A. Bužarovska, S. DinescuA.D. Lazar, M. Serban, G.G Pircalabioru, M. Costache, C. Gualandi, L. Avérous, *Mater. Sci. Eng. C*, **2019**, *104*, 109893.

In this study two series of TPU/BT and TPU/BT_f/$MWCNT_f$ composite films are prepared. The flexibility of TPU and the proper functionalization of $BaTiO_3$ and MWCNTs contributed to increased permittivity and acceptable dielectric breakdown strengths. Despite the high BT loadings, TPU/BT and TPU/BT_f/$MWCNT_f$ composite films are considered as elastic materials with high strength, suitable for energy storage devices.

E. Stojchevska, R. Popeski-Dimovski, Ž. Kokolanski, C. Gualandi*, A.Bužarovska*

Title Effect of Particle Functionalization on Structural and Dielectric Properties of Flexible TPU/$BaTiO_3$/MWCNTs Composite Films

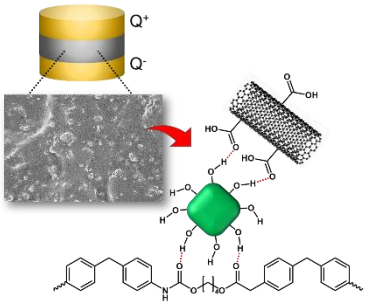

In this study two series of TPU/BT and TPU/BT_f/$MWCNT_f$ composite films are prepared. The flexibility of TPU and the proper functionalization of $BaTiO_3$ and MWCNTs contributed to increased permittivity and acceptable dielectric breakdown strengths. Despite the high BT loadings, TPU/BT and TPU/BT_f/$MWCNT_f$ composite films are considered as elastic materials with high strength, suitable for energy storage devices.